12. Kureychik V.M. Geneticheskie algoritmi i ih primenenie [Genetic algorithms and their application] – Taganrog: TRTU, 2002, - 242 p.

13. Rudkovskaya D., Pilinskiy M., Rudkovskiy L., Neyronie seti, geneticheskie algoritmi I nechetkie mnogistva [Neural networks, genetic algorithms and fuzzy systems] – M.: Hotline – Telecom, 2013. – 384 p.

Sadigov I.R.
Department of Mechanics,
Azerbaijan University of Architecture and Construction,
Ayna Sultanova 11, Baku, Azerbaijan

THE STABILITY OF THIN-WALLED OPEN- PROFILE BARS WITHIN THE NONLINEAR ELASTIC DEFORMATION

Abstract. The paper considers researches dealing with the stability of thin-walled open-profile bars. The widespread use of thin-walled bars in engineering constructions is resulted in a significant reduction in the weight of these systems. Considering the relevance of the given problem, the stability of nonlinear deformation to the central axis direction of the thin-walled bars has been investigated. The physical nonlinearity of the bar's material, dependence of the normal tension in its cross-section on the relative linear deformation has been taken as the form of the dual cubic polynomial. An appropriate nonlinear differential complex equation for a single torsion angle has been composed for the determination of the normal and touching tensions at bar's cuts in the non-free torsion of the longitudinal compression of the bar subjected to nonlinear deformations, and free touch tensions in free torsion towards the direction of the thickness of the bar. In order to use the small parameter method for the solution of this differential equation, the small parameter expression is composed of the elastic characteristics of the bar material. The solution line of the form of the nonlinear differential equation due to the small number of parameters is divided into differential equations, so that their solution is easily carried out. As a result, the expression of thin-walled bar's tension is obtained in the third approximation.

Keywords: Thin-walled bar, nonlinear deformation, open -profile, deplanation, non-free torsion, bending, curling moment, sectorial field, sustainability.

INTRODUCTION

The tap of the thin-walled bars in different constructions, especially in shipbuilding, aviation industry, and construction of high-mile buildings, etc., caused a creation of the new computation theory. The famous scientist, Vlasov's fundamental works had an irreplaceable role in the sphere of the creation and development of this theory [1]. Taking into account that the thin-walled bars squeezed in the longitudinal direction are problematic ones, the significant investigations of Peres N., Goncalves R., Camotim D. and others along with Vlasov's survey had a great impact on their work on calculations for sustainability [2-4, 9].

Unlike the closed contoured or the whole cut thin-walled bars, the open-profile bars are slightly resistant to torsion. According to the general theory of open profile thin-walled bars, in the torsion of such bars their cuts are bent, thus various points take different movements in the direction of the central longitudinal axis of the bar. Such longitudinal displacements are called deplanation.

PROBLEM STATEMENT

If the deplanation of the cuts of the bar doesn't occur freely, it implies that normal tensions arise in non-free torsion. In this case touch tensions also arise in the points of the cut of the bar. These touching tensions are indicated as $\tau^{q.s.}$, they are accepted like regularly disseminated in wall thickness of the shaft [1]. In the free torsion the tensile stresses varying by linear law in the direction of bar thickness are called free touching tensions, and are indicated as τ^{s} (see Fig. 1).

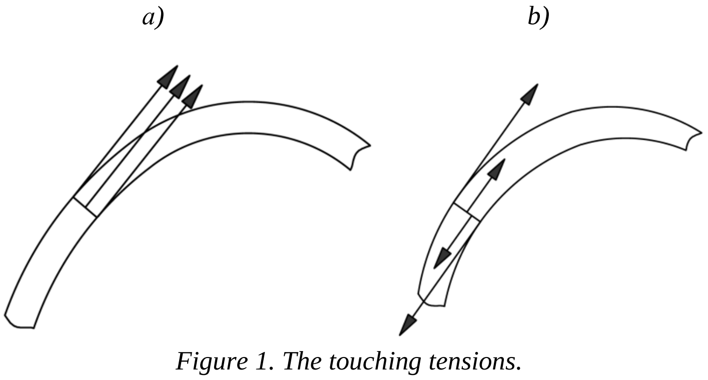

Figure 1. The touching tensions.
Non-free torsion; b) Free torsion

When we indicate the momentum that is born of internal touch forces in the free torsion with $\overline{M}_b$, and the momentum that is born of touch forces in the non-free torsion with $\overline{\overline{M}}_b$, the full torque momentum is taken as follows:

$$M_b = \overline{M}_b + \overline{\overline{M}}_b \qquad (1)$$

The shift (deplanation) u of any point of the cut of the bar to the longitudinal axis x can be taken as follows [2]:

$$u = -\alpha(x)\cdot\omega(s), \qquad (2)$$

here $\alpha(x)-$ is the relative torsional angle of bar, which is the function of x variable, $\omega(s)-$ is the sectorial area of S function. Sectorial area as rotation of radius-vector that takes its beginning from any polar point k is assumed as double area resulting from the movement of the last (the second) point on the middle line of the bar wall (Fig. 2).

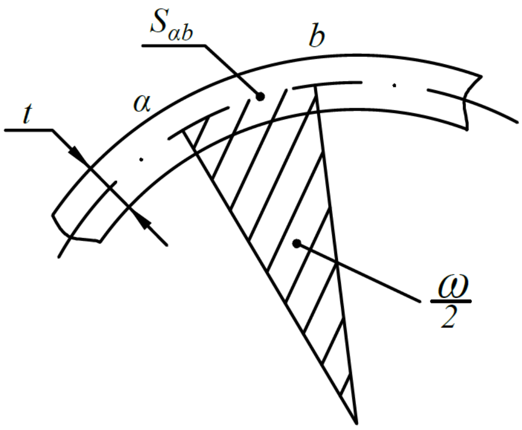

Figure 2. The sectorial area.

The negative symbol in Eq. (2) indicates the counterclockwise rotation of the radius-vector. Considering that the bar material is non-linear elastic, we find normal tension in its most extreme non-free torsion in the cut of the bar as follows [5]:

$$\sigma_x = E_o\varepsilon_x - E_1\varepsilon_x^3, \qquad (3)$$

here $\boldsymbol{E_o, E_1} -$ are elastic constants of the bar material, ε_x is the relative longitudinal linear deformation.

Choosing the Method of Solution

Let's make the last expression as follows:

$$\sigma_x = E_o\varepsilon_x\left(1 - \nu\beta\varepsilon_x^2\right), \qquad (4)$$

here $\boldsymbol{\nu = \frac{E_1}{E_o}\varepsilon^2_{m.h.}} -$ is the small parameter drawn from the elasticity of the bar material $\boldsymbol{(\nu < 1), \beta = 1/\varepsilon^2_{m.h.}, \varepsilon_{m.h.}} -$ is the relative deformity of the material due to the range of the tolerance of the material [6].

Using Koshi dependences and considering Eq. (2), we can write the following:

$$\varepsilon_x = -\frac{d\alpha(x)}{dx}\cdot\omega(s), \qquad (5)$$

here the single torsion angle $\boldsymbol{\alpha(x)}$ equals to derivative of $\boldsymbol{\theta} -$ through x variable:

$$\alpha = -\frac{d\theta}{dx}$$

Taking into account the last equation, we can substitute Eq. (5) with Eq. (4) and have:

$$\sigma_x = -E_o\left[\frac{d^2\theta}{dx^2}\omega(s) - \nu\beta\left(\frac{d^2\theta}{dx^2}\right)^3\cdot(\omega(s))^3\right] \qquad (6)$$

Considering the following equilibrium Eq. (6) we determine the touching tensions:

$\frac{\partial \sigma_x}{\partial x} + \frac{\partial \tau}{\partial s} = 0$, from here

$$\tau = -\int_0^s \frac{\partial \sigma_x}{\partial x} ds = E_o \left[\frac{d^3\theta}{dx^3} \int_0^s \omega ds - \nu\beta \cdot \frac{d}{dx}\left(\frac{d^2\theta}{dx^2}\right)^3 \int_0^s (\omega(s))^3 ds \right] \tag{7}$$

We take the last equation and multiply it with the thickness of the bar wall t and get the intensity of the flood of the forces touching along its wall:

$$\tau t = -\int_0^s \frac{\partial \sigma_x}{\partial x} t ds = E_o \left[\frac{d^3\theta}{dx^3} \int_0^s \omega t ds - \nu\beta \cdot \frac{d}{dx}\left(\frac{d^2\theta}{dx^2}\right)^3 \int_0^s (\omega(s))^3 t ds \right] \tag{8}$$

In Eq. (8) we mark $\boldsymbol{tds = dF}$ and $\boldsymbol{\tau \cdot t = q}$, but integrals are indicated as follows:

$-S_\omega = \int_0^s \omega dF -$ sectorial static momentum (unit of measurement sm^4),

$-J_\omega = \int_0^s \omega^2 dF -$ sectorial inertial momentum (unit of measurement sm^6).

Considering these signs, we make Eq. (8) in the following form [7]:

$$q = E_o \left[\frac{d^3\theta}{dx^3} S_\omega - \nu\beta \cdot \frac{d}{dx}\left(\frac{d^2\theta}{dx^2}\right)^3 \cdot \int_F \omega^3 dF \right] \tag{9}$$

We define the $\overline{\overline{M}}_b$ momentum due to arrow passing through the k pole of the tensile forces in the non-free torsion. As it is seen from Fig. 3, sm^6 is polar momentum of elemental force $\boldsymbol{q\rho ds = q \cdot d\omega}$ (here $\boldsymbol{d\omega = \rho ds}$ – is the growth of the sectorial area).

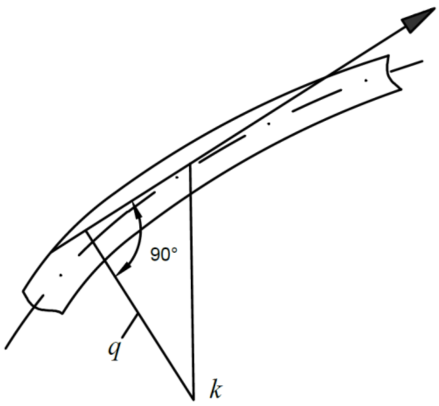

Figure 3. Determination of momentum of the touched force.

Momentum alternative $\overline{\overline{M}}_b$ is written as follows:

$$\overline{\overline{M}}_b = \int_F q d\omega = E_o \left[\frac{d^3\theta}{dx^3} \int_F d\omega \int_F \omega dF - \nu\beta \cdot \frac{d}{dx}\left(\frac{d^2\theta}{dx^2}\right)^3 \cdot \int_F d\omega \int_0^s \omega^3 dF \right],$$

here integration is carried out on all F areas.
We get this equation through partial integration:

$$\overline{\overline{M}}_b = E_o\left[\frac{d^3\theta}{dx^3}\left(\omega\int_F \omega dF - J_\omega\right) - \nu\beta\cdot\frac{d}{dx}\left(\frac{d^2\theta}{dx^2}\right)^3\cdot\left(\omega\int_F \omega^3 dF - \int_F \omega^4 dF\right)\right] \quad (10)$$

In the definition of the sectorial area the starting position of the radius-vector is determined by the fact that the exact sectorial static momentum of the field is zero, that is:

$$S_{\omega.F} = \int_F \omega dF = 0 \quad (11)$$

Realization of the Method

Taking into consideration the above-mentioned symbols, we put Eq. (10) in this form:

$$\overline{\overline{M}}_b = -E_o\left[J_\omega\cdot\frac{d^3\theta}{dx^3} - \nu\beta\cdot\frac{d}{dx}\left(\frac{d^2\theta}{dx^2}\right)^3\cdot\left(\omega\int_F \omega^3 dF - \int_F \omega^4 dF\right)\right] \quad (12)$$

We can write the momentum of the tensile forces of the profile that are created by the free torsion as follows:

$$\overline{M}_b = GJ_k\cdot\frac{d\theta}{dx} \quad (13)$$

here GJ_k is rigidity of profile in torsion, J_k is inertia momentum of torsion. We can write the equation in the following way (if profile consists of rectangle):

$$J_k = \frac{1}{3}\eta\sum_{i=1}^{n} s_i\cdot t_i^3, \quad (14)$$

here S_i is the length of the *i* small wall, t_i is the thickness, and η – is the ratio that is the basis of the shape of the cut. The unit of J_k measurement is sm^4.

According to Eq. (1) the general torsional momentum equals to the sum of Eq. (12) and Eq. (13):

$$M_b = -E_o\left[J_\omega\cdot\frac{d^3\theta}{dx^3} - \nu\beta\cdot\frac{d}{dx}\left(\frac{d^2\theta}{dx^2}\right)^3\cdot\left(\omega\int_F \omega^3 dF - \int_F \omega^4 dF\right)\right] + GJ_k\frac{d\theta}{dx} \quad (15)$$

This equation (Eq. 15) is the nonlinearial differential equation of the non-free torsion of the open profile thin-walled bar.

Let's express touching forces with the following new *B(x)* function of the momentum of the torsional forces in non-free torsion:

$$\frac{dB}{dx} = \overline{\overline{M}}_b \quad (16)$$

here *B* is called bending – torsional bimoment (bumper), or simply bimoment, its unit of measurement is $kN\text{-}sm^2$.

In the process of comparing Eq. (6) and Eq. (12) we get:

$$\overline{\overline{M}}_b = \frac{d\sigma_x}{dx}\cdot\frac{J_\omega}{\omega} \quad (17)$$

While comparing Eq. (16) and Eq. (17) we get:

$$\sigma_x = \frac{B\cdot\omega}{J_\omega} \quad (18)$$

We can see from here that, the normal tensions in the non-free torsion are proportional to the bimoment, and while it is $\boldsymbol{\sigma_x = 0}$, $\boldsymbol{B = 0}$ is obtained.

Placing Eq. (16) in Eq. (12) we integrate according to *x* and get the following:

$$B = -E_o\left[J_\omega \cdot \frac{d^2\theta}{dx^2} - \nu\beta\left(\frac{d^2\theta}{dx^2}\right)^3 \cdot \left(\omega\int_F \omega^3 dF - \int_F \omega^4 dF\right)\right] \tag{19}$$

We differentiate both sides of Eq. (15) according to x and get:

$$E_o\left[J_\omega \cdot \frac{d^4\theta}{dx^4} - \nu\beta \cdot \frac{d^2}{dx^2}\left(\frac{d^2\theta}{dx^2}\right)^3 \cdot \left(\omega\int_F \omega^3 dF - \int_F \omega^4 dF\right)\right] - GJ_k\frac{d^2\theta}{dx^2} = \frac{dM_b}{dx} = m_b, \tag{20}$$

Here m_b is the intensity of the external bending forces and we accept it as a positive quantity, because M_b decreases while the value of *x* increases.

First of all, let's look at the existence form of the two symmetry arrows of the bar cut (double-headed form) (Fig. 4, a). Such bar with length of *l* is influenced by the squeezing *P* force in the direction of the centre axis *x* [7].

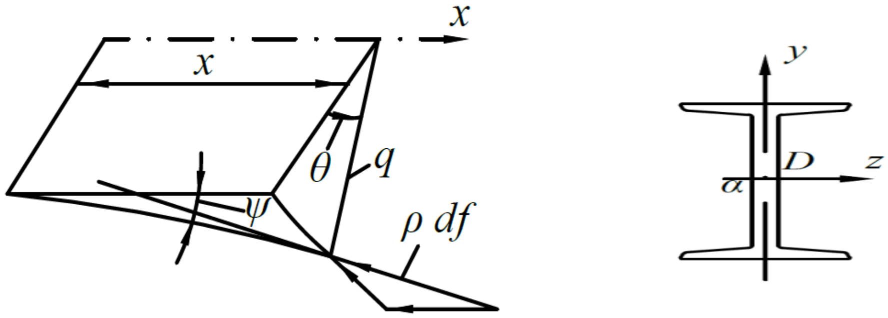

D-the centre of bending

Figure 4. a) Double-headed cut; b) About computing the torque of the squeezing force.

Let's assume that all the longitudinal fibers except the central fibers are bending from the given force (to the direction of *x* arrow), i.e. the form of the loss of the tolerance in the torsion of the bar. When looking through the free edge of the bar at the *x* arrow we accept that the positive direction of the $\boldsymbol{\theta}$ rotation angle of any cut of the bar is turning counterclockwise [8].

Before deformation, accepting the fact that *dF* elemental pitch fits to any fiber in the cut of the bar parallel to *x* axis, after the torsion the bending radius of the very fiber will have the curve shape on the surface of the $\boldsymbol{\rho}$ circular cylinder (Fig. 4, b). Let's mark the vertical fiber and angle of the touch to this curve with $\boldsymbol{\psi}$. The $\boldsymbol{\sigma \cdot dF}$ elemental force that effects the fiber is spinning like $\boldsymbol{\psi}$ angle, creating the momentum around the *x* arrow, will also be expressed as $\boldsymbol{\sigma\psi\rho dF}$, and the intensity of the full torque momentum will be expressed as follows:

$$m_b = -\int_F \sigma\frac{d\psi}{dx}\rho\, dF, \tag{21}$$

or considering that $\boldsymbol{\rho d\theta = \psi dx}$ it will be like:

$$m_b = -\sigma\frac{d^2\theta}{dx^2}\int_F \rho^2\, dF = -\sigma\frac{d^2\theta}{dx^2}J_p, \tag{22}$$

here J_p is the polar inertia momentum due to the centre of the cut. Writing Eq. (22) for Eq. (20), we get the following nonlinear differential equation [10,11]:

$$E_o\left[J_\omega \cdot \frac{d^4\theta}{dx^4} - \nu\beta \cdot \frac{d^2}{dx^2}\left(\frac{d^2\theta}{dx^2}\right)^3 \cdot \left(\omega\int_F \omega^3 dF - \int_F \omega^4 dF\right)\right] + \left(\sigma J_p - GJ_k\right)\frac{d^2\theta}{dx^2} = 0, \quad (23)$$

We solve this complex differential equation by using the small parameters method. For this purpose we put Eq. (23) in the following form:

$$\frac{d^4\theta}{dx^4} - \nu\frac{\beta}{J_\omega} \cdot \frac{d^2}{dx^2}\left(\frac{d^2\theta}{dx^2}\right)^3\left(\omega\int_F \omega^3 dF - \int_F \omega^4 dF\right) + \frac{\sigma \cdot J_p - GJ_k}{E_o J_\omega} \cdot \frac{d^2\theta}{dx^2} = 0 \quad (23')$$

We take the solution of the last equation in the following order for a small parameter:

$$\theta = \theta_o + \nu\theta_1 + \ldots = \sum_{n=0}^{\infty} \nu^n \theta_n \qquad (n \geq 0) \quad (a)$$

We write (a) in the same equation and obtain the following linear differential equation system (the first two equations of the system were shown):

$$\frac{d^4\theta_o}{dx^4} + \frac{\sigma_{b(o)} \cdot J_p - GJ_k}{E_o J_\omega} \cdot \frac{d^2\theta_o}{dx^2} = 0 \quad (24)$$

$$\frac{d^4\theta_1}{dx^4} + \frac{\sigma_{b(o)} \cdot J_p - GJ_k}{E_o J_\omega} \cdot \frac{d^2\theta_1}{dx^2} = \frac{\beta}{J_\omega} \cdot \frac{d^2}{dx^2}\left(\frac{d^2\theta_o}{dx^2}\right)^3\left(\omega\int_F \omega^3 dF - \int_F \omega^4 dF\right) \quad (25)$$

The following substitution was accepted in Eq. (24):

$$\frac{\sigma_{b(o)} \cdot J_p - GJ_k}{E_o J_\omega} = k_o^2, \quad (26)$$

We obtain its solution through the following way:

$$\frac{d^2\theta_o}{dx^2} = C_1 \sin k_o x + C_2 \cos k_o x \quad (27)$$

Since the boundary conditions are

$$C_2 = 0, C_2 \neq 0$$

we get $\boldsymbol{\sin k_o l = 0; k_o l = n\pi}$ or $\boldsymbol{k_o = \frac{n\pi}{l}}$

Accepting n=1, we write $\boldsymbol{k_o = \pi/l}$ in Eq. (26) and find the initial cost of the crisis tension:

$$\sigma_{b(o)} = \frac{\pi^2 E_o J_\omega}{l^2 J_p} + \frac{GJ_k}{J_p}, \quad (28)$$

Similarly to the strongest fasteners of the sharpest ends of the bars, we can write Eq. (28) in the following way:

$$\sigma_{b(o)} = \frac{\pi^2 E J_\omega}{(\mu l)^2 J_p} + \frac{GJ_k}{J_p}, \quad (28')$$

Here the length coefficient of the bar may be equal to $\boldsymbol{\mu = 0{,}5}$. If one of the cutting edges of the bar is tightly fastened and the other one is rolling $\boldsymbol{\mu = 0{,}7}$ is accepted.

Taking into account $\boldsymbol{C_2 = 0}$, Eq. (27) takes the following form:

$$\frac{d^2\theta_o}{dx^2} = C_1 \sin k_o x \tag{29}$$

Considering Eq. (29), the following complex differential in Eq. (25) is defined as:

$$\frac{d^2}{dx^2}\left(\frac{d^2\theta_o}{dx^2}\right)^3 = C_1^3\left(-\frac{3}{4}k_o^2 \sin k_o x + \frac{9}{4}k_o^2 \sin 3k_o x\right) \tag{30}$$

Subsequenty, placing Eq. (30) in Eq. (25) we get:

$$\frac{d^4\theta_1}{dx^4} + k_1^2 \cdot \frac{d^2\theta_1}{dx^2} = \frac{\beta}{J_\omega} C_1^3 \cdot \left(-\frac{3}{4}k_o^2 \sin k_o x + \frac{9}{4}k_o^2 \sin 3k_o x\right)^3 \left(\omega \int_F \omega^3 dF - \int_F \omega^4 dF\right) \tag{31}$$

here

$$k_1^2 = \frac{\sigma_{b(1)} \cdot J_p - GJ_k}{E_o J_\omega} \tag{32}$$

we accept the solution of the differential in Eq. (31) in the following way:

$$\frac{d^2\theta_1}{dx^2} = D_1 \sin k_1 x + D_2 \cos k_1 x + C_1^3 k_o^2 (a \sin k_o x + b \sin 3k_o x) \cdot \frac{\beta}{J_\omega}\left(\omega \int_F \omega^3 dF - \int_F \omega^4 dF\right) \tag{33}$$

by substituting Eq. (33) in Eq. (25), we get equations *a* and *b*:

$$a = -\frac{3}{4} \cdot \frac{1}{\alpha_k^2 - 1}, \quad b = \frac{9}{4} \cdot \frac{1}{\alpha_k^2 - 1}, \tag{34}$$

here

$$\alpha_k = \frac{k_1}{k_o}$$

Let's assume that the cutting edges of the bar do not rotate in the flat shape. In this case, the boundary conditions of the equation will be as follows:

$$\left.\begin{aligned} &\boldsymbol{x = 0, \quad x = l \quad olduqda \quad \theta = 0;} \\ &\boldsymbol{x = 0, \quad x = l \quad olduqda \quad \frac{d\theta}{dx} = 0} \end{aligned}\right\} \tag{35}$$

We write Eq. (29) and Eq. (33) equations to their places in expression *a* and get :

$$\frac{d^2\theta}{dx^2} = \frac{d^2\theta_o}{dx^2} + v\frac{d^2\theta_1}{dx^2} = C_1 \sin k_o x + \\ + v\left[D_1 \sin k_1 x + C_1^3 k_o^2 (a \sin k_o x + b \sin 3k_o x)\frac{\beta}{J_\omega}\left(\omega \int_F \omega^3 dF - \int_F \omega^4 dF\right)\right] \tag{36}$$

We get the last equation by integrating it:

$$\frac{d\theta}{dx}=\frac{d\theta_o}{dx}+v\frac{d\theta_1}{dx}=-\frac{C_1}{k_o}\cos k_o x-$$

$$-v\left[\frac{1}{k_1}D_1\cos k_1 x+C_1^3 k_o^2\left(\frac{a}{k_o}\cos k_o x+\frac{b}{3k_o}\cos 3k_o x\right)\frac{\beta}{J_\omega}\left(\omega\int_F \omega^3 dF-\int_F \omega^4 dF\right)\right];$$

$$\theta=\theta_o+v\theta_1=-\frac{C_1}{k_o^2}\sin k_o x-v\left[\frac{1}{k_1^2}D_1\sin k_1 x+C_1^3\left(a\cdot\sin k_o x+\frac{b}{9}\sin 3k_o x\right)\cdot\right.$$

$$\left.\cdot\frac{\beta}{J_\omega}\left(\omega\int_F \omega^3 dF-\int_F \omega^4 dF\right)\right] \tag{37}$$

Substituting Eq. (37) in the boundary conditions of Eq. (35), we get:

$$\left.\frac{d\theta}{dx}\right|_{x=0}=0;\quad -\frac{C_1}{k_o}-v\left[\frac{D_1}{k_1}+C_1^3 k_o\left(a+\frac{b}{3}\right)\cdot\frac{\beta}{J_\omega}\left(\omega\int_F \omega^3 dF-\int_F \omega^4 dF\right)\right]=0;$$

$$\left.\frac{d\theta}{dx}\right|_{x=l}=0;\quad \frac{C_1}{k_o}\cos k_o l+v\left[\frac{D_1}{k_1}\cos k_1 l+C_1^3 k_o\left(a\cos k_o l+\frac{b}{3}\cos 3k_o l\right)\cdot\right.$$

$$\left.\cdot\frac{\beta}{J_\omega}\left(\omega\int_F \omega^3 dF-\int_F \omega^4 dF\right)\right]=0;$$

$$\theta|_{x=0}=0;$$

$$\theta|_{x=l}=0;\quad -\frac{C_1}{k_o^2}\sin k_o l-v\left[\frac{D_1}{k_1^2}\sin k_1 l+C_1^3\left(a\sin k_o l+\frac{b}{9}\sin 3k_o l\right)\cdot\right.$$

$$\left.\cdot\frac{\beta}{J_\omega}\left(\omega\int_F \omega^3 dF-\int_F \omega^4 dF\right)\right]=0 \tag{38}$$

From the first of the conditions of Eq. (38) we get:

$$C_1^3=-\frac{\dfrac{C_1}{k_o}+v\dfrac{D_1}{k_1}}{vk_o\dfrac{\beta}{J_\omega}\left(a+\dfrac{b}{3}\right)\cdot\left(\omega\int_F \omega^3 dF-\int_F \omega^4 dF\right)} \tag{39}$$

Having written the last expression in the place of other conditions of Eq. (38), we obtain the following algebric equations for C_1 and D_1 constants:

$$\frac{C_1}{k_o}\left(\cos k_o l-\frac{a\cdot\cos k_o l+\frac{b}{3}\cos 3k_o l}{a+\frac{b}{3}}\right)+v\frac{D_1}{k_1}\left(\cos k_1 l-\frac{a\cdot\cos k_o l+\frac{b}{3}\cos 3k_o l}{a+\frac{b}{3}}\right)=0$$

$$\frac{C_1}{k_o^2}\left(\sin k_o l-\frac{a\cdot\sin k_o l+\frac{b}{9}\sin 3k_o l}{a+\frac{b}{3}}\right)+v\frac{D_1}{k_1^2}\left(\sin k_1 l-\frac{a\cdot\sin k_o l+\frac{b}{9}\cos 3k_o l}{a+\frac{b}{3}}\right)=0 \quad (40)$$

Making the Eq. (40) system's determinant equal to zero for getting the smallest value of the k_1, we obtain the following complex algebraic equations system:

$$\frac{1}{k_1^2 k_o}\left(\cos k_o l-\frac{a\cos k_o l+\frac{b}{3}\cos 3k_o l}{a+\frac{b}{3}}\right)\left(\sin k_1 l-\frac{a\sin k_o l+\frac{b}{9}\sin 3k_o l}{a+\frac{b}{3}}\right)+$$

$$+\frac{1}{k_o^2 k_1}\left(\sin k_o l-\frac{a\sin k_o l+\frac{b}{9}\sin 3k_o l}{a+\frac{b}{3}}\right)\left(\cos k_1 l-\frac{a\cos k_o l+\frac{b}{3}\cos 3k_o l}{a+\frac{b}{3}}\right)=0$$

Defining the minimum equation for the coefficient k_1 through numerical methods from the last equation and writing it in Eq. (32) we determine the crisis tension - $\boldsymbol{\sigma_{b(1)}}$ in the first approach:

$$\boldsymbol{\sigma_{b(1)}=\frac{k_1^2 E_o J_\omega+GJ_k}{J_p}} \quad (41)$$

Analogically, as described above, by keeping the first two boundaries of the expression ($\boldsymbol{a}$) and having written in the differential Eq. (23′) we get appropriate $\boldsymbol{k_2=2\pi/l}$ coefficient, and the crisis tension $\boldsymbol{\sigma_{b(2)}}$ according to the $\boldsymbol{n=2}$ condition of the small parameter, i.e. due to $\boldsymbol{v^2-a}$. Thus, we determine the crisis tension in the second approximation of thin-walled bar:

$$\boldsymbol{\sigma_b^{(II)}=\sigma_{b(0)}+v\sigma_{b(1)}+v^2\sigma_{b(2)}} \quad (42)$$

Numerous calculations have shown that, the difference between the sum of the first two limits of Eq. (42) and ($\boldsymbol{\sigma_b^{(I)}}$ – the first approximation) the second approximation is 1,64%. Therefore we can be satisfied with that the equation can be solved by the solution in the second approach.

CONCLUSION

The problem of clamping resistance in the centre of the thin-walled open profile bars has been extensively studied. For the first time, the nonlinear elastic property of the material of the bars is taken into account, in addition, the nonlinear differential equilibrium equation for the determination of crisis tension has been compiled. The smallest parameters method, which is most optimal for determining the crisis tension in the differential equation, has been used. As a result, the complex nonlinear differential equation is divided into several simple linear differential equations and their solution provides the satisfactory results specially in the second approximation.

References

[1] Vlasov V. Thin-walled elastic beams.2nd ed. Springfield, Va.: National Technical Information Service; 1984.

[2] Peres N, Goncalves R, Camotim D. First-order generalized beam theory for curved thin-walled members with circular axis. Thin-Walled Structures 2016; vol.107: 345-361. DOI: 10.1016/j.tws.2016.06.016

[3] Fouzi MSM. Jelani KM. Nazri NA. Sani MSM. Finite Element Modelling and Updating of Welded Thin-Walled Beam. International Journal of Automotive and Mechanical Engineering 2018; 15(4): 5874-5889. DOI: 10.1007/s40430-018-1475-z

[4] Bebiano R, Eisenberger M, Camotim D, Goncalves R. GBT-Based Buckling Analysis Using the Exact Element Method. International Journal of Structural Stability and Dynamics 2017; 17(10): 17501255. DOI: 10.1142/s0219455417501255

[5] Ronaldo I, Borja. Plasticity. Springer, Berlin; 2013.

[6] Rousselier G, Quilici S. Combining porous plasticity with Coulomb and Portevin-Le Chatelier models for ductile fracture analyses. International Journal of Plasticity 2015; vol.69: 118-133. DOI: 10.1016/j.ijplas.2015.02.008

[7] Walter L. Nonlinear Structural Mechanics: Theory, Dynamical Phenomena and Modeling. Springer US; 2013.

[8] Leipholz U. Theory of elasticity, Springer Netherlands; 2014.

[9] Pastor MM, Bonada J, Roure F, Casafont M. Residual stresses and initial imperfections in non-linear analysis. Engineering Structures 2013; vol.46:493-507. DOI: 10.1016/j.engstruct.2012.08.013

[10] Sadigov IR Phisical nonlinear elastic deformations of smooth ring. Transactions of NAS of Azerbaijan 2016; vol. 36:74–80.

[11] Zhang RJ, Wang C, Zhang Q. Response analysis of the composite random vibration of a high-speed elevator considering the nonlinearity of guide shoe. Journal of the Brazilian Society of Mechanical Sciences and Engineering 2018; vol.40: 4.

УДК 626.627.8

Абилов Рашад Саффан оглы,
докторант, научной сотрудник,
Азербайджанский Научно-Исследовательский и
Проектно-Изыскательный Институт Энергетики,
лаборатория «Источники альтернативной энергии и
малые электрические станции»
г. Баку, Азербайджан

РАЗРАБОТКА И СОВЕРШЕНСТВОВАНИЕ КОНСТРУКЦИИ ОТСТОЙНИКА ДЛЯ ГИДРОЭНЕРГЕТИКИ И ИРРИГАЦИИ

Abilov Rashad Saffan oglu,
Doctoral student, researcher,
Azerbaijan Scientific-Research and Design Institute of Surveying Energy,
laboratory of «alternative energy sources and small power stations»
Baku, Azerbaijan

DEVELOPMENT AND IMPROVEMENT OF THE SEDIMENT DESIGN FOR HYDRO-POWER ENGINEERING AND IRRIGATION

Аннотация. В статье рассматриваются и анализируются различные типы отстойников (по конструктивным схемам, по режиму потока), изучена динамика осаждения и способом промывки наносов. Даны рекомендации по использованию в гидроэнергетике и ирригации разных конструкций отстойников.

Abstract. Different types of sedimentation basins are considered and analyzed in the article on constructive schemes, the flow regime, the dynamics of sedimentation and the method of washing of sediments, and the recommended improvement for hydropower and irrigation of various sedimentation tanks have been studied.

Ключевые слова: потоки, осаждения, наносы, элементы, конструкции, ирригация, частицы.

Key words: flows, sediments, deposits, elements, structures, irrigation, particles.

Очистка воды методом отстаивания применяется на гидросооружениях, в системах централизованного водоснабжения и канализации.

Отстойники представляют собой резервуары или открытые емкости, в которых методом отстаивания удаляются из воды механические примеси. В ходе этого процесса частицы дисперсионной фазы в зависимости от плотности вещества либо всплывают на поверхность воды, либо оседают на дно резервуара. Частицы, осевшие на дно, образуют осадок. В ряде случаев осаждение сопровождается укрупнением частиц. Отстаивание воды является довольно распространенным способом удаления грубодисперсных механических примесей. Этот метод применяется в системах гидроузлов, централизованного водоснабжения и канализации, на ГЭС, ирригационных сооружениях, а также при очистке коммунальных сточных вод и после биологической очистки стоков [2, 3].

На насосных станциях и ГЭС поступающие воды из открытых источников подвергаются отстаиванию для того, чтобы предотвратить истирание лопастей гидротурбин и частей насосов твердыми примесями размером более 0,25 мм. Применение отстойников в ирригационных системах целесообразно, чтобы не допустить засорения илом оросительных каналов.

В системах централизованного водоснабжения отстойники применяются на водоочистных станциях, для предварительного осветления воды с